Molecular Vision 2020; 26:392-408 <http://www.molvis.org/molvis/v26/392>
Received 10 November 2019 | Accepted 1 June 2020 | Published 3 June 2020

Protective effect of magnesium acetyltaurate against NMDA-induced retinal ganglion cell loss in rats involves calcium-regulated proteins

Azliana Jusnida Ahmad Jafri,[1] Renu Agarwal,[2] Igor Iezhitsa,[1,3,4] Puneet Agarwal,[2] Nafeeza Mohd Ismail[2]

[1]Center for Neuroscience Research, Faculty of Medicine, Universiti Teknologi MARA Sungai Buloh Campus, Selangor, Malaysia; [2]School of Medicine, International Medical University, Kuala Lumpur, Malaysia; [3]Volgograd State Medical University, Research Centre for Innovative Medicines, Volgograd, Russian Federation; [4]Institute for Pathology, Laboratory and Forensic Medicine (I-PPerForM), Universiti Teknologi MARA, Sungai Buloh Campus, Selangor, Malaysia

Purpose: NMDA receptor overactivation has been implicated in the apoptotic loss of retinal ganglion cells (RGCs) in glaucoma, the leading cause of irreversible blindness. Excessive influx of Ca^{2+} after stimulation of the N-methyl-D-aspartate (NMDA) receptors in RGCs results in activation of several Ca^{2+}-regulated proteins that include calpain-1, cabin-1, and CaMKII. Interactions of these Ca^{2+}-regulated proteins triggers RGC apoptosis. Previous studies have shown that a compound consisting of magnesium and taurine, magnesium acetyltaurate (MgAT), protects against NMDA-induced retinal and optic nerve injury in rats. However, whether these effects of MgAT involve Ca^{2+}-regulated proteins remains unclear. Therefore, in the present study, we investigated whether the protective effect of MgAT against NMDA-induced RGC loss is associated with its action on Ca^{2+}-regulated proteins.

Methods: Sprague-Dawley rats were intravitreally injected with NMDA with or without pre-treatment with MgAT. Seven days later, the animals were euthanized, and the retinas were isolated to determine the expression of calpain-1, cabin-1, and CaMKII proteins and genes using western blotting and PCR, respectively. The extent of RGC survival was determined using Brn3A immunostaining and retrograde labeling of RGCs using FluoroGold. Furthermore, before the animals were euthanized, the rats' visual functions were examined using an open-field arena and the Morris water maze test.

Results: It was observed that NMDA exposure resulted in RGC apoptosis and poor visual functions. These effects of NMDA were associated with significantly greater expression of the calpain-1 and CaMKII genes and proteins, whereas those for cabin-1 were significantly lower. NMDA also caused greater phospho-CaMKII expression indicating its activation. Pretreatment with MgAT protected against NMDA-induced changes in the expression of calpain-1, cabin-1, CaMKII, and phospho-CaMKII. These effects of MgAT were associated with greater RGC survival and preservation of visual functions.

Conclusions: It could be concluded that MgAT protects against NMDA-induced loss of RGCs and visual functions via its effects on the expression of calpain-1, cabin-1, and CaMKII in rat retinas.

Glaucoma is the leading cause of irreversible blindness. The vision loss in glaucoma is characteristically associated with retinal ganglion cell (RGC) apoptosis [1,2]. Excitotoxicity is one of the mechanisms involved in RGC apoptosis, and it involves excessive stimulation of glutamate receptors [3]. Glutamate is the major excitatory neurotransmitter in the central nervous system and retina, and is required for physiologic functions. However, excessive accumulation of glutamate within synapses is neurotoxic due to the excessive stimulation of the glutamate receptors [4]. Glutamate receptors are largely divided into ionotropic and metabotropic receptors. The ionotropic receptors include N-methyl-D-aspartate (NMDA) receptors, α-amino-3-hydroxyl-5-methyl-4-isoxazole-propionate (AMPA) receptors, and kainic acid receptors, each of which is sensitive to a specific glutamate analog [5]. Among the three ionotropic receptors, predominantly, the overstimulation of NMDA receptors is known to mediate RGC apoptosis due to their extreme permeability to Ca^{2+} [6]. Exposure to exogenous NMDA causes rapid RGC degeneration as the cells abundantly express NMDA receptors [7]. For this reason, animal models of NMDA-induced retinal damage have been used for research related to excitotoxicity-induced neurodegeneration and evaluation of neuroprotective strategies [8,9].

Intracellular Ca^{2+} overload after stimulation of the NMDA receptor initiates several apoptotic pathways. Although the precise molecular events involved in Ca^{2+}-dependent apoptotic loss of RGCs remain unclear, activation of calpain-1, cabin-1, calcineurin (Cn), and calcium calmodulin kinase II (CaMKII) has been widely investigated.

Correspondence to: Renu Agarwal, School of Medicine, International Medical University, Kuala Lumpur, Malaysia, Phone: +60361265000; email: renuag02@gmail.com

Calpains are a family of calcium-dependent cytoplasmic cysteine proteases that are ubiquitously present in mammalian cells [10]. The proteases have been proposed to influence signal transductions and mediate cell death by targeting several key cytoskeletal and membrane proteins, as well as enzymes [11]. Among the several calpain substrates, Cn, cabin-1, and CaMKII are important Ca^{2+}-regulated proteins and have widely been investigated for their role in neuronal apoptosis. Cn, a phosphatase, consists of two subunits, CnA (a 60-kDa catalytic subunit) and CnB (a 19-kDa regulatory subunit). CnB has the Ca^{2+} binding site whereas CnA binds with calmodulin. Calmodulin binding causes cleavage and release of the autoinhibitory domain and activates the enzymatic activity of CnA [12]. Studies have shown that calpain-induced cleavage of CnA in the presence of excitotoxicity leads to neuronal degeneration [13]. Recent studies identified a Ca^{2+}-regulated protein, cabin-1, that has a Cn binding domain and is important in regulating Cn activity. Binding of cabin-1 with Cn causes inactivation of Cn; thus, cabin-1 is regarded as an endogenous inhibitor of Cn. Cabin-1 is also a calpain substrate. In the presence of Ca^{2+} overload, the cleavage of cabin-1 by calpain renders it inactive leading to Cn activation and subsequent cell damage [14]. Activation of retinal Cn after stimulation of the NMDA receptors is well described; however, the effects on cabin-1 expression in the retina remain unknown. Another Ca^{2+}-dependent multifunctional serine-threonine protein kinase that is known to have a role in excitotoxicity-mediated RGC apoptosis is CaMKII. Its presence has been detected in inner nuclear and ganglion cell layers [15]. It is activated when an increase in intracellular Ca^{2+} leads to binding of the Ca^{2+} and CaM complexes. The activation of CaMKII is implicated in various neuronal functions [16]. Multiple studies have also shown that it mediates signal transduction leading to excitotoxicity-induced neuronal apoptosis [17-19].

In addition, NMDA-induced excitotoxicity in RGCs is associated with increased nitrosative and oxidative stress [20,21]. In previous studies, we observed that pretreatment with magnesium acetyltaurate (MgAT), a combined salt of Mg and taurine, prevents NMDA-induced retinal and optic nerve damage, and this protective effect of MgAT involved reduction in oxidative and nitrosative stress in rat retinas [22,23]. It was proposed that because Mg is a known NMDA antagonist, and taurine also antagonizes Ca^{2+} channels, MgAT reduces retinal oxidative and nitrosative stress by reducing the intracellular Ca^{2+} influx subsequent to NMDA exposure. However, it remains unknown whether pretreatment with MgAT affects the NMDA-induced activation of Ca^{2+}-regulated proteins. Therefore, in this study we investigated the effect of MgAT pretreatment on NMDA-induced changes in retinal gene and protein expression for calpain-1, cabin-1, and CaMKII. We also investigated whether the effect of MgAT on the expression of these genes and proteins is associated with increased RGC survival and improved visual functions in rats.

METHODS

The study was conducted in accordance with the ARVO Statement for Use of Animals for Ophthalmic and Vision Research and the animal ethics guidelines of Universiti Teknologi MARA (Malaysia). Accordingly, in the pilot study, all intravitreal injections were administered unilaterally. In the main study, however, the rats were subjected to functional assessment, and thus, bilateral injections were administered. Sprague-Dawley rats of either sex, aged 8–12 weeks (200–250 g), were procured from the Laboratory Animal Care Unit, Universiti Teknologi MARA. The animals were housed under standard laboratory conditions of 12-h:12-h light-dark cycles. Food and water were available ad libitum. All animals were subjected to general and ophthalmic examinations, and those with no abnormalities were included in the study.

Study design: The study design consisted of a preliminary pilot study to determine the effects of MgAT alone on RGC survival. The pilot study consisted of two groups of six animals each. One of the groups received PBS (1X; 1 mM KH_2PO_4, 155 mM $NaCl_2$, 2 mM Na_2HPO_4-$7H_2O$, pH 7.4) intravitreally in one of the randomly chosen eyes, whereas the other eye remained untreated. The other group similarly received MgAT 320 nM dissolved in PBS. The intravitreal injections were administered in a total volume of 2 µl as described previously [22-26]. All rats in both groups were subjected to retrograde labeling of RGCs using FluoroGold, which was injected on day 1 after treatment using stereotaxis. On day 7 after treatment, the rats were euthanized with an intraperitoneal injection of pentobarbital (100 mg/kg). Retinal flatmounts were examined to determine the density of the FluoroGold-stained cells. A comparison of the FluoroGold-stained RGC density between the untreated and treated eyes within a group did not show statistically significant differences. A comparison of RGC density between the PBS- and MgAT-injected eyes also did not show statistically significant differences (Figure 1).

The pilot study was followed by the main study. In the main study, among the three groups of animals comprising 132 animals each, groups 1 and 2 were treated with PBS and NMDA, respectively. Group 3 received MgAT as pretreatment 24 h before NMDA. NMDA was injected at a dosage of 160 nM, whereas MgAT was injected at double the equimolar dose of NMDA (320 nM) as reported previously [22,24]. In

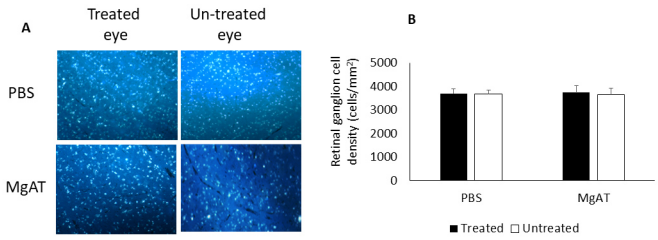

Figure 1. Effect of MgAT alone on RGC survival as assessed by retrograde labelling of RGCs using fluorogold in a pilot study. **A**: Representative pictures of retinal flatmounts showing fluorogold stained RGCs. **B**: Quantitative estimation of the RGC density. Rats were treated unilaterally and intravitreally with either PBS or MgAT. No significant differences were observed between treated and untreated eyes within groups. Additionally, no differences were observed between PBS and MgAT treated eyes.

this study, we excluded the group treated with MgAT alone because in the pilot study it was observed that MgAT did not affect the RGC survival, and the effects of MgAT were comparable to those of PBS. All treatments were given bilaterally and intravitreally in a total volume of 2 µl as described previously [22-26].

In each group, a set of 30 animals each was sacrificed as previously stated, at 3, 6, and 24 h and 7 days after treatment. The eyes were enucleated, and the retinas were isolated after the anterior segment and vitreous were carefully removed. The retinas were homogenized and subjected to western blotting to detect expression of calpain-1, cabin-1, total CaMKII, and phospho-CaMKII proteins. PCR was performed to the detect the gene expression for *calpain-1, cabin-1, CaMKII-α, CaMKII-β, CaMKII-δ,* and *CaMKII-γ.* For each parameter, two retinas from the same animal were pooled and used as one sample. Each parameter was determined using three biological samples. Each biological sample was subjected to three technical replicates in each group.

To assess the extent of RGC survival, another set of six rats from each group was subjected to retrograde labeling of RGCs for which FluoroGold was injected on day 1 after-treatment using stereotaxis. Subsequently, on day 7 after the injection these rats were euthanized as previously stated. Retinal flatmounts were prepared to determine the RGC count.

To assess the visual functions, a set of six rats from each group was subjected to training for visual functions tests starting on the day of injection for 5 days. Visual functions tests using an open-field arena and the Morris water maze test were conducted on day 6 after the injection. On day 7 after the injection, the animals were euthanized as previously stated, and the eyes were enucleated with a suture placed at the 12 o'clock position and subjected to Brn3A immunostaining to further assess the extent of RGC survival in various groups.

Immunoblotting: Western blotting was performed using the whole retinal extracts. The enucleated eyes were bisected at the equator, and the lenses were removed. The retinas were peeled off carefully using forceps under a surgical microscope and were washed with PBS (pH 7.4) three times, to remove any adhered vitreous. The retinal tissue was homogenized in 50 µl of radioimmunoprecipitation assay (RIPA) buffer at 4 °C by sonication for 1 min. The supernatant was collected, and the total protein concentration was determined using A280 NanoDrop (Thermo Scientific Inc., Waltham, MA). The lysates were centrifuged at 5,000 ×*g* for 15 min at 4 °C. The protein samples were run on 10% to 12% sodium dodecyl sulfate-polyacrylamide gel electrophoresis (SDS–PAGE; 25 µg of the total protein was added to each lane), transferred to nitrocellulose membranes (Schleicher and Schuell GmbH, Einbeck, Germany), and then incubated with the appropriate primary antibody. The following primary antibodies were used for immunoblotting: mouse monoclonal anti-Calpain-1; (1:1,000; Santa Cruz Biotechnology, Dallas, TX), mouse monoclonal anti-cabin-1 (1:1,000; Santa Cruz Biotechnology), mouse monoclonal anti-CaMKII (1:1,000; Santa Cruz Biotechnology), mouse monoclonal phospho-CaMKII (1:1,000; Santa Cruz Biotechnology), and mouse monoclonal beta-actin (1:1,000; Santa Cruz Biotechnology). After incubation at 4 °C overnight, the membranes were washed. The membranes were further incubated with horseradish peroxidase (HRP) conjugated goat anti-mouse secondary antibody (1:1,000; Santa Cruz Biotechnology) for 2 h at room temperature and visualized using a working solution of equal amounts of stable peroxidase and enhancer solution. For the densitometric analysis, specific bands were normalized to the β-actin protein level.

Quantitative real-time PCR: Total RNA was extracted from the isolated retinas using the GeneJET™ RNA Purification Kit (Thermo Scientific, Inc., Rockford, IL), which utilizes a silica-based membrane technology in the form of convenient spin columns. Using the RapidOut DNA Removal

kit (Thermo Scientific, Inc.), genomic DNA was removed from the total RNA. Before quantitative real-time PCR (qPCR) was performed, RNA purity and concentration were determined by using an automated capillary electrophoresis system, Agilent 2100 Bioanalyzer (Agilent, Waldbronn, Germany). Total RNA analysis was done using the Agilent RNA 6000 Nano Kit (Agilent). The Maxima® First Strand cDNA Synthesis Kit (Thermo Scientific, Inc.) was used to prepare cDNA from the RNA. Experiments with qPCR were designed according to the MIQE guidelines [27] using Luminaris Color HiGreen qPCR Master Mix (Thermo Scientific, Inc.). The thermal cycling profile of the BioRad iCycler PCR machine was set according to the manufacturer's protocol, and the reactions were run for 45 cycles. All PCR reactions were performed in triplicate. Standard curves were made for each reference gene and gene of interest to calculate the PCR efficiencies. The ΔΔCT method was used to determine the relative fold expression of the genes of interest, and the data were normalized to the reference genes *GAPDH* and β-actin (*ACTB*). Primer specificity was confirmed with Nucleotide Basic Local Alignment Search Tool (BLAST). All primers were supplied by Sigma Aldrich Life Science (St. Louis, MO) and are presented in Table 1.

Retrograde labeling of RGCs: To assess the extent of RGC survival, RGCs were retrogradely labeled with FluoroGold (Santa Cruz Biotechnology) as described previously. Briefly, the rats were anesthetized with an intraperitoneal injection of a mixture of ketamine (80 mg/kg) and xylazine (8 mg/kg), and then the heads of the rats were fixed in a stereotaxic apparatus (Stoelting Co., Wood Dale, IL). A 2-cm incision was made on the scalp, and a hole was drilled using a surgical drill at 7 mm posterior to the bregma, 2 mm lateral to the midline, and up to a depth of 4.0 mm from the bone surface on both sides avoiding any injury to the meninges. A total volume of 1 µl of 4% FluoroGold solution prepared in distilled water was injected into each hole using a Hamilton syringe (Hamilton, Bonaduz, Switzerland) mounted on the stereotactic frame. After each injection, the needle was left in place for 1 min to avoid reflux of the solution [28,29]. Seven days after the injection, the rats were euthanized, and the eyes were enucleated. The enucleated eyes were fixed in 4% paraformaldehyde overnight at room temperature. Subsequently, using a surgical microscope (OPMI pico; Carl Zeiss, Jena, Germany), the whole retinal cup was isolated, and a flower-shaped retinal flatmount was prepared by making four cuts at the periphery of the retina to flatten it. The flatmounts were examined under a fluorescence microscope (Olympus Ix8; Olympus Scientific Corporation, Tokyo, Japan) using a rhodamine filter at 515 nm. Live RGCs were visualized as fluorescent dots. For quantification, three microscopic fields of 120 × 160 µm^2 in each quadrant were chosen to count the labeled RGCs. The first image was taken at 0.875 mm from the optic disc, and the remaining two were 1 mm apart from each other (Figure 2). Then, the density of the labeled cells in the 12 photographs was averaged and expressed as the mean density of FluoroGold-positive RGCs per square millimeter of retina.

Brn3A immunostaining: Paraffin-embedded retinal tissue was sectioned at 1 mm from the temporal edge of the optic disc and subjected to dehydration and rehydration. The retrieval of antigen was performed in 10 mM, 0.05% Tween-20, pH 6.0 of sodium citrate at boiling point for 20 min in a domestic microwave. The incubation with monoclonal Brn3A primary antibody (Santa Cruz Biotechnology) was done overnight at 4 °C. Incubation with HRP conjugated secondary antibody (Santa Cruz Biotechnology; 2:98) diluted with tris buffer saline (TBS) with 1% bovine serum albumin (BSA) was performed for 1 h at room temperature. After 1 h, the slides were washed, developed with chromogen, and counterstained with hematoxylin. Finally, the sections were dehydrated, mounted, and observed under the light microscope (Leica Microsystem, Wetzlar, Germany) at 20X magnification. Three sections from each retina were evaluated and in each section, three randomly chosen fields of vision were used to count the Brn3A-stained cells by two independent observers.

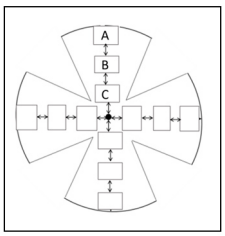

Figure 2. Diagrammatic representation of the retinal flatmount showing areas of RGC count. Three microscopic fields (120 x 160 µm^2) in each quadrant were chosen to count labelled RGCs. Area labelled "C" was 0.875 mm from the optic disc. The distance between areas **A**, **B**, and **C** was 1 mm.

The average was expressed as Brn3A-positive cells/100 μm^2 of the ganglion cell layer (GCL) [30].

Visual function tests: To determine the rats' visual functions, color recognition tests were performed using an open-field arena and the Morris water maze test. The protocol for these tests was designed to maximize the testing for visual ability and minimize the contribution of memory and is described below.

Open-field test and color recognition test in open-field arena: The open-field test was used to measure the rats' exploratory and anxiety-related behavior as part of the animal stress response associated with visual loss. In a soundproof room, the open-field arena made from an expanded polyvinyl chloride (PVC) square arena 100 cm (L) × 70 cm (H) × 100 cm (W) was used. The whole arena was subdivided into peripheral (10,000 cm^2 each 100 cm (L) × 100 cm (W)) and central (2,500 cm^2 each 50 cm (L) × 50 cm (W)) zones and was illuminated with a 100-W tungsten lamp. A specialized small camera was installed on top of the apparatus showing the whole arena field. Observations were done in four steps.

First, the observation started when the rats were placed individually in the center area and were allowed to explore the entire area for 10 min while a camera attached on top recorded the behavior. During each 10-min period, the total distance traveled, the number of squares crossed, frequency of grooming, total immobility time and number of immobility episodes, and frequency of rearing (frequency with which the rat stood on its hind legs in the field) were recorded.

After 10 min, the rat was removed, and the arena was wiped with 75% ethanol to clean the rat urine and feces. This was to avoid the transmission of olfactory cues and prevent rats from smelling and staying at the same position. After the cleaning process, two colored bottles (blue and green, identical in size and shape) were placed diagonally in the arena. The rat was placed again for 10 min. After 10 min, the rat and the colored bottles were removed, and the arena was cleaned again. This was the familiarization phase. Once the arena was cleaned, two blue bottles were placed diagonally in the arena, and the rat was placed again. This was the color displacement phase. Once again, the arena was cleaned. Then, instead of two blue bottles, two green bottles were similarly placed in the arena, and the rat was allowed to explore for 10 min. This phase was the color cue replacement phase. Each rat sequentially went through the four phases each day, and this made up one complete trial. The rats underwent four such trials with trial 1 on the day after the NMDA injection (experimental day 2) and trial 4 on experimental day 5. After four trials, on day 6 of experiment, the rats were subjected to testing which consisted of exactly the same four phases, and the rats' exploratory activities were recorded. All observations were analyzed using ANY-maze software (Stoelting Co.; Figure 3).

Color recognition test using the Morris water maze test: The Morris water maze test is widely used to study spatial memory and learning. The protocol for the experiment was designed to minimize the contribution of memory in color recognition. In the Morris water maze test, the animals are required to find the submerged platform to escape from swimming in a pool of water using a distal, visual cue at the periphery of the pool as described previously [31]. Briefly, rats are placed in a pool of water that was made opaque by adding a non-toxic coloring agent. Due to the opaque color, the rats are not able to see the platform to escape from the water, and they have to rely on the external or extra maze cues provided. This method developed by Morris in 1981 is considered the gold standard for a visual behavior study as

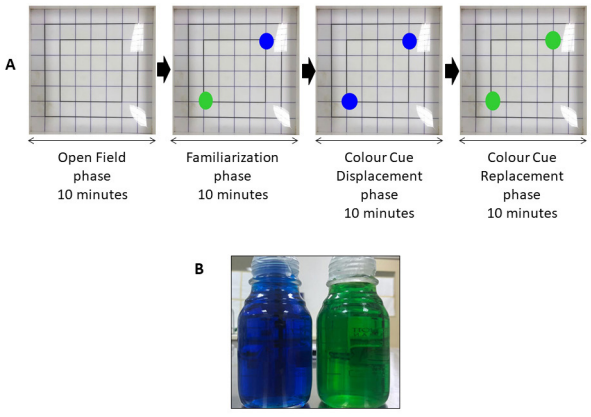

Figure 3. Experimental design for color recognition test in open field arena. **A**: 4 phases in the test protocol. In each phase, rat was placed alone and the rat movement was recorded for 10 min. **B**: Color cues used for the visual function test in Open Field Arena.

the recognition of the platform depends not only on memory but also on the visual cues.

Thus, in the present study the rats' visual recognition ability was evaluated using the water maze test as previously described by Morris [32] with Vorhees and Williams' (2006) and Nunez's modifications [33,34]. The experiments were performed in a circular tank with a diameter of 150 cm and a height of 60 cm. In the present study, we paired the submerged platform only with the blue card, and not the green card, so that recognition would not be dependent on memory alone but also on the visual cues (Figure 4). The water temperature was maintained at 25 ± 1 °C. The experiment is described in Figure 3 and began with a 4-day training session as was the case with open-field test (starting from the day after the NMDA injection until day 5 of the experiment). The rats recognized the platform that was elevated 1 inch from the water surface in any of the quadrants but always paired with the color cue (blue) attached on the wall of the pool. The rat was placed in all four quadrants rotationally. In the training session, the rats learned how to find the platform within 60 s with the help of the cue. After training, all rats were subjected to the visual recognition test during which the platform remained submerged. Both color cues were displayed; however, the platform was paired with only the blue cue. The time taken by the rats to find the platform was recorded and analyzed with the ANY-maze software (Stoelting Co.).

Statistical analysis: All data are expressed as mean ± standard deviation (SD). Statistical analysis was performed using one-way analysis of variance (ANOVA) followed by Bonferroni post hoc analysis for multiple comparisons using SPSS. A p value of less than 0.05 was considered statistically significant. For the visual function tests, the data were analyzed using the Kruskal-Wallis test using SPSS. A p value of less than 0.05 was considered statistically significant.

RESULTS

Effect of MgAT pretreatment on NMDA-induced changes in the retinal expression of the calpain-1, cabin-1, and CaMKII proteins: Estimation of calpain-1 protein expression using western blotting showed a trend toward greater expression in the NMDA-treated group compared to the corresponding PBS-treated group. Densitometric analysis showed 1.55- and 1.58-fold greater expression of calpain-1 in the NMDA-treated group compared to the corresponding PBS-treated group at 24 h and 7 days after treatment, respectively ($p<0.05$ and $p<0.01$, respectively). In the MgAT-pretreated group, calpain-1 expression was lower than in the corresponding NMDA-treated group by 1.60- and 2.27-fold at the same time points, respectively ($p<0.05$ and 0.01, respectively; Figure 5).

The lower retinal expression of the cabin-1 protein was evident in the NMDA-treated group compared to the corresponding PBS-treated group at all time points, and densitometric analysis showed that the difference totaled to 2.08-, 2.01-, 1.60-, and 1.33-fold at 3, 6, and 24 h and 7 days after treatment, respectively. The MgAT-pretreated group showed higher levels of cabin-1 protein expression compared to the corresponding NMDA-treated group ($p<0.05$; Figure 6).

Retinal expression of the CaMKII protein was also determined using western blotting at 3, 6, and 24 h and 7 days after treatment. The total CaMKII expression was greater in the NMDA-treated group compared to the corresponding PBS-treated group at 24 h and 7 days after treatment, and the difference was 2.15- and 2.78-fold, respectively ($p<0.05$ and $p<0.001$, respectively). At the same time points, the expression of the CaMKII protein in the MgAT-pretreated group was lower than that in the corresponding NMDA-treated

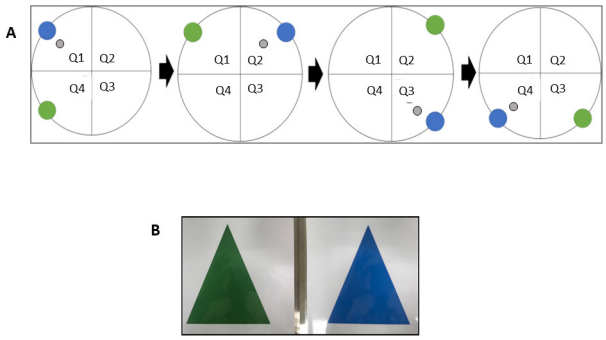

Figure 4. Experimental Protocol for Morris Water Maze Test. **A**: Placement of platform was paired with colored cue in any of the 4 quadrants. The blue color cue was placed in the same quadrant as the platform during training. The grey circle in quadrant indicates the platform changing its position in different quadrant every 60 s. **B**: The colors cues used in this experiment.

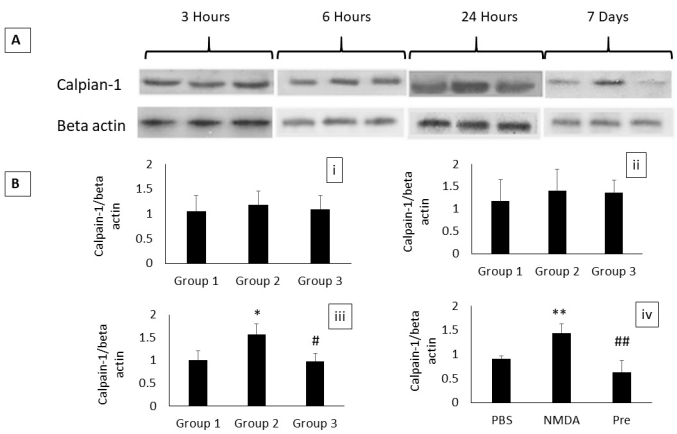

Figure 5. Effect of MgAT pre-treatment on NMDA-induced changes in the retinal calpain-1 expression. **A**: Calpain-1 and β actin bands obtained from Western blot at 3-, 6-, 24-h and 7 days post-treatment. **B**: The densitometric analysis of Western blot bands (i) 3 h after treatment (ii) 6 h after treatment (iii) 24 h after treatment (iv) 7 days after treatment. Group 1 was injected with PBS, group 2 was injected with NMDA and group 3 was injected with MgAT 24 h before the injection of NMDA. *p<0.05 versus group 1, **p<0.01 versus group 1, #p<0.05 versus group 2, ##p<0.01 versus group 2. N=3 for each time point.

group and there was a 1.55- and to 2.16-fold difference, respectively (p<0.05 and p<0.001, respectively). At 6 h and the subsequent time points, the densitometric analysis showed the presence of phosphorylated CaMKII protein in the NMDA-treated group. However, the presence of the phosphorylated CaMKII protein was not detected in either the PBS- or MgAT-pretreated group at any time point (Figure 7).

Effect of MgAT pretreatment on NMDA-induced changes in the retinal expression of the calpain-1, cabin-1, and CamKII genes: The retinal expression of the *calpain-1 gene* in the NMDA-treated group was upregulated at 6 h after treatment by as much as 3.08-fold compared to the corresponding PBS-treated group (p<0.001). At 24 h and 7 days after treatment as well, the NMDA-treated group showed significant upregulation of the expression of the *calpain-1 gene* compared to the corresponding PBS-treated group with a 1.41- and 1.44-fold difference (p<0.001 and p<0.05, respectively). In the MgAT-pretreated group, the *calpain-1 gene* was significantly downregulated compared to the corresponding NMDA-treated group at 3, 6, and 24 h after treatment, and the difference was 3.22-, 1.90-, and 1.90-fold, respectively (p<0.001; Figure 8).

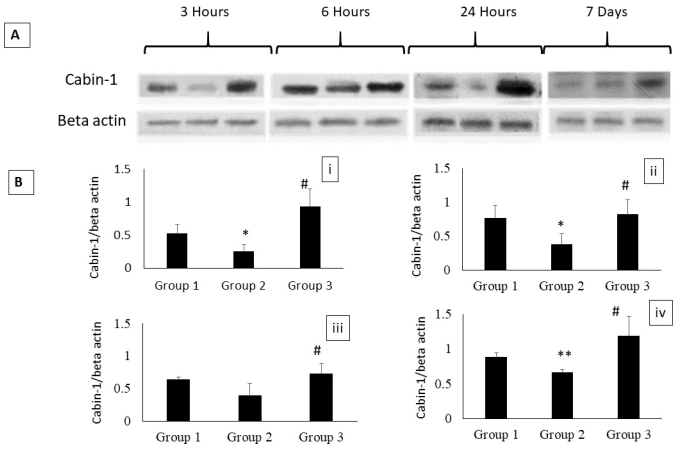

Figure 6. Effect of MgAT pre-treatment on NMDA-induced changes in the retinal cabin-1 expression. **A**: Cabin-1 and β actin bands obtained from Western blot at 3-, 6-, 24-h and 7 days post-treatment. **B**: The densitometric analysis of Western blot bands (i) 3 h after treatment (ii) 6 h after treatment (iii) 24 h after treatment (iv) 7 days after treatment.. Group 1 was injected with PBS, group 2 was injected with NMDA and group 3 was injected with MgAT 24 h before the injection of NMDA. *p<0.05 to group 1, **p<0.01 to group 1, #p<0.05 to group 2. N=3 for each time point.

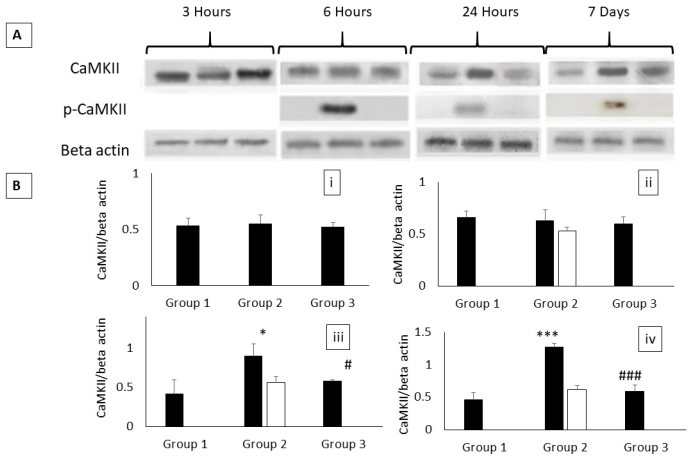

Figure 7. Effect of MgAT pre-treatment on NMDA-induced changes in the retinal CaMKII expression. **A**: Total CaMKII, phospho-CaMKII and β-actin bands obtained from Western blot at 3-, 6-, 24-h and 7 days post-treatment. **B**: The densitometric analysis of Western blot bands (i) 3 h after treatment (ii) 6 h after treatment (iii) 24 h after treatment (iv) 7 days after treatment. Group 1 was injected with PBS, group 2 was injected with NMDA and group 3 was injected with MgAT 24 h before the injection of NMDA. *<0.05 versus group 1, ***p<0.001 versus group 1, #p<0.05 to group 2, ###p<0.001 versus group 2. N=3 for each time point.

The expression of the *cabin-1 gene* in the NMDA-treated group was conspicuously downregulated by 4.52-, 1.78-, 4.71-, and 1.51-fold at 3 h (p<0.001), 6 h (p<0.001), 24 h (p<0.001), and 7 days (p<0.001) respectively, after treatment compared to the corresponding PBS-treated group. In contrast, the expression of the *cabin-1 gene* in the MgAT-pretreated group was upregulated at 3 h (p<0.001), 6 h (p<0.001), 24 h (p<0.001), and 7 days (p<0.01) after treatment compared to the corresponding NMDA-treated group, and the differences were 3.93-, 1.89-, 3.76-, and 1.05-fold, respectively (Figure 8).

The expression of all four isoforms of *CaMKII*, including *CaMKII-α*, *CaMKII-β*, *CaMKII-γ*, and *CaMKII-δ*, was upregulated in the NMDA-treated group compared to the corresponding PBS-treated group. Expression of *CaMKII-α*, *CaMKII*-β, and *CaMKII*-δ at 3 h after treatment remained comparable to that in the corresponding PBS-treated group; however, CaMKII-γ showed significantly greater expression compared to the corresponding PBS-treated group at this time point (p<0.05). At 6 h after treatment, the genes for all four isoforms of *CaMKII* were significantly upregulated in the NMDA-treated group compared to the corresponding PBS-treated group (p<0.001). Similarly, at 24 h and 7 days after treatment all four genes remained significantly upregulated in the NMDA-treated group compared to the PBS-treated group. The MgAT-pretreated group showed lower expression of *CaMKII*-α, *CaMKII*-β, and *CaMKII*-δ at all time points compared to the NMDA-treated group. The expression of the *CaMKII*-γ *gene* was significantly lower in the MgAT-pretreated group compared to the corresponding NMDA-treated group at 6 h, 24 h, and 7 days after treatment (p<0.001; Figure 9).

Effect of MgAT on NMDA-induced loss of RGCs:

Brn3A immunostaining—In the present study, Brn3A immunostaining was also performed to quantify RGC

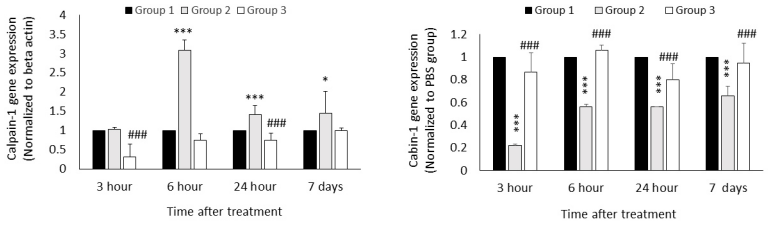

Figure 8. Effect of MgAT on NMDA-induced changes in retinal gene expression of (**A**) calpain-1 (**B**) cabin-1 at 3-, 6-, 24-h and 7 days post-treatment. Group 1 was injected with PBS, group 2 was injected with NMDA and group 3 was injected with MgAT 24 h before the injection of NMDA. *p<0.01 versus group 1, ***p<0.001 versus group 1, ###p<0.001 versus group 2. N=3 for each time point.

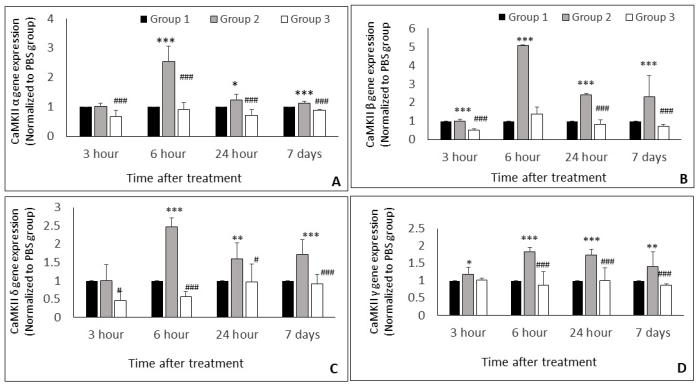

Figure 9. Effect of MgAT on NMDA-induced changes in retinal gene expression of (**A**) CaMKIIα (**B**) CaMKIIβ (**C**) CaMKIIδ and (**D**) CaMKIIγ at 3-, 6-, 24-h and 7 days post-treatment. Group 1 was injected with PBS, group 2 was injected with NMDA and group 3 was injected with MgAT 24 hour before the injection of NMDA. *p<0.05 versus group 1, **p<0.01 versus group 1, ***p<0.001 versus group 1, #p<0.05 versus group 2, ###p<0.001 versus group 2. N=3 for each time point.

survival. Immunohistochemistry showed the statistically significant presence of Brn3A-positive cells in the PBS- and MgAT-treated groups. In contrast, the NMDA-treated group did not show the presence of many Brn3A-positive cells in the GCL. These findings on retinal photomicrographs were further confirmed with a quantitative analysis. Accordingly, the number of Brn3A-positive cells was significantly lower in the NMDA-treated group compared to the PBS-treated group, but in the MgAT-pretreated group, the number was greater than in the NMDA-treated group (p<0.01; Figure 10).

Retrograde labeling of RGCs—The effect of the treatment with MgAT on the extent of RGC survival against NMDA-induced apoptosis was determined with retrograde labeling of RGCs using FluoroGold. Whole retina flatmounts were examined. In the PBS-treated group, numerous fluorescent labeled cells were seen (3,832.215 ± 200.4000), whereas in the NMDA-treated group (1,365 ± 216.9) the number of labeled fluorescent cells was nearly 50% lower than in the PBS-treated group (p<0.001). The MgAT-pretreated group (3,663.368 ± 652.9000) showed numerous fluorescent labeled cells in a pattern similar to that in the PBS group across whole retinas. Quantitatively, the number of labeled RGCs was greater in the MgAT-pretreated group compared to the NMDA-treated group (p<0.001; Figure 10).

Effect of MgAT on NMDA-induced changes in visual functions:

Open-field test and color recognition test—The open-field test is an experiment used to study anxiety- and stress-related behavior in rats. In the present study, several

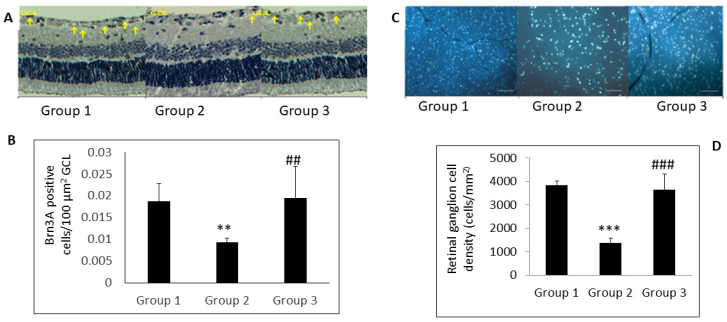

Figure 10. Effect of MgAT on NMDA-induced changes in RGC survival. **A**: Photomicrographs Showing the Brn3A staining of retinal sections (20X). Dark brown cells represent Brn3A positive cells indicating live RGCs (indicated by arrows). **B**: Quantitative estimation of the Brn3A positive cells (n=6). **C**: Retinal flatmounts showing fluorogold stained RGCs. **D**: Quantitative estimation of the density of fluroglod positive cells (n=6). Group 1 was injected with PBS, group 2 was injected with NMDA and group 3 was injected with MgAT 24 hour before the injection of NMDA. NMDA: N-methyl-D-aspartic acid, MgAT: Magnesium Acetyltaurate, GCL: Ganglion cell layer. **p<0.01 versus group 1, ***p<0.001 versus group 1; ##<0.01 versus group 2; ###<0.001 versus group 2. (n=6).

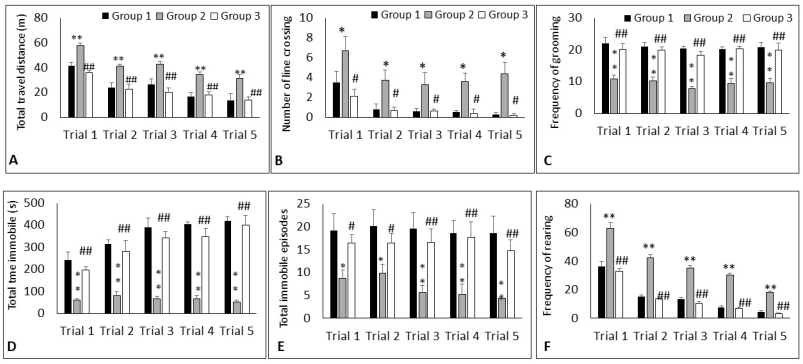

Figure 11. Effect of MgAT on NMDA-Induced changes in the behaviour of rats in open field arena. **A**: Total distance travelled. **B**: Number of line crossing. **C**: Frequency of grooming. **D**: Total immobility time. **E**: Total immobility episodes. **F**: Frequency of rearing. Group 1 was injected with PBS, group 2 was injected with NMDA and group 3 was injected with MgAT 24 hour before the injection of NMDA. NMDA: N-methyl-D-aspartic acid, MgAT: Magnesium Acetyltaurate. *p<0.05 versus group 1, **p<0.01 versus group 1, #p<0.05 versus group 1, ##p<0.01 versus group 2. (n=6).

parameters were used to assess the overall anxiety-related behavior of the rats. On the first day of training, it was observed that the total distance traveled by rats receiving NMDA (group 2) was significantly greater (57 m) compared to the group receiving PBS that traveled 41 m (group 1; p<0.01). The MgAT-pretreated group showed a significantly lower total distance traveled (36 m) compared to the NMDA-treated group (p<0.001). With continued training over 4 days, the rats became familiar with the arena, and the total distance traveled by the rats decreased in all three groups; however, it remained significantly greater in rats treated with NMDA compared to those treated with either PBS or MgAT. In accordance with this observation, throughout the experimental period the number of line crossings and the number of rearing episodes remained significantly greater, and grooming activity remained lower, in the NMDA-treated group compared to the groups treated with either PBS or MgAT. Additionally, the immobility time and the episodes of immobility were significantly smaller in the NMDA-treated group compared to the PBS-treated group indicating the restlessness and anxiety among rats in this group. However, the rats in the MgAT-pretreated group showed significantly greater immobility time and episodes compared to the NMDA-treated group (p<0.01). Last, the rats' frequency of rearing was also recorded. Rearing in behavioral studies is defined as the movement of the animal around the environment attempting to be in contact with stimuli; the head is elevated to investigate the stimuli. Although the rearing activity slowly decreased from trial 1 to trial 5, the animals in the NMDA-treated group continued to show significantly high rearing activity compared to the PBS-treated group (p<0.01). The MgAT-pretreated group showed significantly less rearing activity than the NMDA-treated group (p<0.01) throughout the experimental period (Figure 11).

In the color recognition test, the familiarization phase is a phase in which the rat was placed alone in an open-field arena with two color cues: blue and green. During this phase, the behavior of the rats in terms of the number of times they touched the color cues were analyzed over 10 min. Then, in the spatial test (the displacement and replacement phase), the ability to recognize color cues was measured by estimating the exploration time for 10 min. In the spatial test, the NMDA-treated group showed a longer exploration time for the blue cue compared to the PBS-treated group (p<0.01), and the MgAT-pretreated group showed a shorter exploration time than the NMDA-treated group (p<0.01). However, for the green cue, no differences were observed among the groups (p>0.05; Figure 12A).

Morris water maze test—The rats' color recognition ability was further tested using the Morris water maze test. It was observed that on day 1, the latency period to find the submerged platform was comparable among all three groups. During trials 1, 2, 3, and 4, the rats in the NMDA-treated group took longer to find the platform; thus, the latency period in this group was greater than in the PBS-treated group. Trial 5 represents the test day when the platform was submerged. For this trial, the latency period to find the platform was 1.43-fold greater in the NMDA-treated group than in the PBS-treated group (p<0.05). The MgAT-pretreated group showed a shorter latency period compared to the NMDA-treated group on trial 4 as well as trial 5 (test day; p<0.01; Figure 12B,C).

DISCUSSION

The present study was performed to elucidate the mechanisms underlying the protective effect of MgAT pretreatment against NMDA-induced RGC apoptosis in Sprague-Dawley rats. Retrograde labeling of RGCs with FluoroGold and Brn3A immunostaining clearly demonstrated that NMDA-induced loss of RGCs is attenuated by pretreatment with MgAT. The RGC loss caused by NMDA exposure was associated with increased gene and protein expression of calpain-1 and CaMKII, whereas the expression of cabin-1 was reduced. The protective effect of MgAT was associated with reduced gene and protein expression of calpain-1 and CaMKII, and increased expression of cabin-1. Additionally, it was observed that pretreatment with MgAT protected against the NMDA-induced changes in the rats' visual behavior.

The key triggering event in NMDA-mediated excitotoxicity is the intracellular influx of Ca^{2+} which activates several Ca^{2+}-regulated pathways culminating in RGC apoptosis. Calpain activation results in the activation of substrates carrying calpain cleavage sites, such as calcineurin, cabin-1, caspase 12, BID, and Bax, and leads to apoptosis [35]. The calpains exist in two prototypical forms, calpain-1 (μ-calpain), and calpain-2 (m-calpain). Calpain-1 is activated by micromolar concentrations of calcium and is located in the cytosol or near the membranes. Calpain-2, located at the membranes, requires millimolar concentrations of calcium for activation [36]. Although the physiological concentrations of calcium range from 100 to 1,000 nM [37], excitotoxicity causes the concentration to increase to 5−10 μM [38]. Selective coupling of calpain-1 activation with NMDA receptor excitotoxicity has previously been demonstrated [39,40]. In accordance with these observations, the present study showed a statistically significant increase in retinal calpain-1 expression at 24 h and 7 days after exposure to NMDA. This result, however, was in contrast to a previous study that showed increased calpain-1 expression much earlier at 6 h and 12-h after NMDA injection [40]. It has been proposed that calpain-1 activation by NMDA is often a late event as it occurs downstream of mitochondrial involvement in excitotoxicity [41]. In this regard, after the initial Ca^{2+} influx following NMDA exposure, neurons try to reestablish the intracellular Ca^{2+} levels by pumping back into the extracellular compartment as well as by mitochondrial uptake [42]. Continued increase in intracellular Ca^{2+} beyond the buffering capacity causes excessive activation and expression of Ca^{2+}-dependent proteins that leads to apoptosis [43]. This may also be the reason for the relatively late detection of increased calpain-1 expression. In the present study, MgAT seems to antagonize the NMDA receptors and reduce the Ca^{2+} influx, culminating in reduced expression of calpain-1.

One of the significant results in the present study is the effect of MgAT on cabin-1 expression. MgAT pretreatment was associated with significantly high cabin 1 protein expression at all four time points after treatment compared to the NMDA treatment group. In line with this observation, *cabin-1 gene* expression was also higher in the MgAT-treated group compared to the NMDA-treated group at all time points and at 24 h and 7 days after treatment. It was even greater than in the PBS-treated group indicating profound cellular response to MgAT treatment against NMDA insult. Although increased cabin-1 expression was noted at earlier

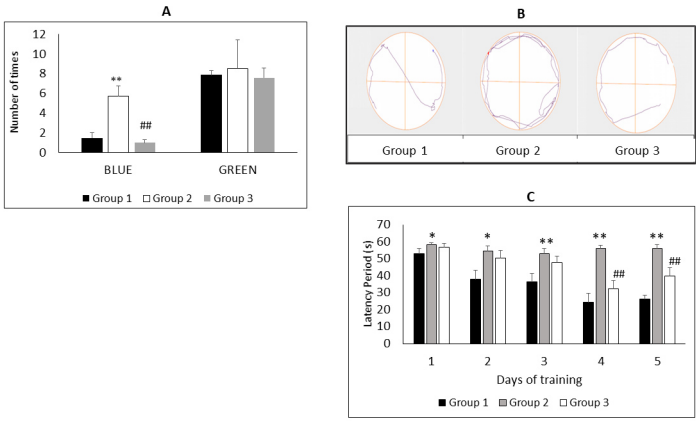

Figure 12. Effect of MgAT on NMDA-Induced changes in the colour recognition by rats. **A**: Colour recognition test in open field arena (**B**) track plot of the activity of rats in Morris Water Maze for 60 s. **C**: Latency period for rats to find the platform in Morris Water Maze. Group 1 was injected with PBS, group 2 was injected with NMDA and group 3 was injected with MgAT 24 h before the injection of NMDA. NMDA: N-methyl-D-aspartic acid, MgAT: Magnesium Acetyltaurate. *p<0.05 versus group 1, **p<0.01 versus group 1, ##p<0.01 versus group 2. (n=6).

time points of 6 and 12 h, it is likely that its activation occurs only after calpain-1 is activated at 24 h and 7 days after treatment. It can be speculated that in the present study, cleavage of cabin-1 from Cn by Ca^{2+}-activated calpain in the NMDA-treated group triggered the Cn-mediated cell death. After cleavage, cabin-1 could no longer inhibit Cn, and thus, the activated Cn led to cell death. A recent study showed that cabin-1 inhibits Cn activity by inhibiting binding of CnA with CnB by binding with its CnB binding domain. It may also inhibit calpain-dependent truncated CnA activity of 48-kDa and 45-kDa fragments [13,14]. The most impressive evidence discovered to show cabin-dependent Cn activity was that cabin-1 and Cn have strikingly similar localization in the brain where both proteins occur exclusively in the neurons [44].

This study also determined the protein and gene expression of another Ca^{2+}-regulated protein, CaMKII. CaMKII is a target for Ca^{2+} and CaM complex binding, and this binding triggers autophosphorylation of its Thr286, Thr305, and Thr306 resulting in its activation [45,46]. CaMKII activation has been shown to contribute to the death of neuronal cells, including RGCs resulting in visual dysfunction [47-50], whereas inhibition of CaMKII activation is neuroprotective [51]. In the present study, expression of all four genes encoding for four isoforms of CaMKII proteins was determined. However, at the protein level total CaMKII was detected using western blotting because CaMKII, which is made up of 12 subunits, may comprise multiple isoforms [52,53]. In accordance with findings in previous studies, NMDA exposure in this study caused upregulation of the expression of all four isoforms of the *CaMKII* genes, and accordingly, the protein expression increased at 24 h and 7 days after NMDA exposure. These effects of NMDA on CaMKII gene and protein expression were effectively antagonized in the MgAT-pretreated group. Importantly, phospho-CaMKII expression indicating activation of CaMKII was evident in the NMDA-treated group but was not detected in the MgAT-pretreated group indicating the ability of MgAT to inhibit the expression as well as the activation of CaMKII. Activated CaMKII causes mitochondrial Ca^{2+} overload, release of cytochrome c, and activation of caspase 3 leading to apoptosis [54]. Moreover, the role of CaMKII is important not only for mediating NMDA-induced neuronal apoptosis via caspase activation but also because it perpetuates NMDA excitotoxicity. CaMKII phosphorylates the protein PSD95, which protects NMDA receptors against proteolysis and dysregulation by calpain-1. By phosphorylating PSD95, CaMKII terminates its protective action against calpain-induced changes in NMDA receptor action [55]. Therefore, MgAT-induced suppression of the expression and activation of CaMKII is likely to reduce RGC apoptosis by reducing caspase activation, as well by preventing PSD95 phosphorylation. Previous studies demonstrated that MgAT protects against NMDA-induced retinal caspase-3 activation [21,23].

An overview of the effects of MgAT on the expression of three Ca^{2+}-regulated proteins observed in this study allows synthesis of possible molecular events that were triggered by NMDA and were antagonized by MgAT. It appears that the influx of Ca^{2+} triggered by NMDA exposure resulted in increased calpain-1 expression that triggers cabin-1 release from calcineurin resulting in calcineurin activation, which promotes neuronal apoptosis. Ca^{2+} influx also resulted in CaMKII activation, which not only triggered apoptosis but also perpetuated the dysfunction of NMDA receptors further enhancing the excitotoxic injury. The observations made on Brn3A immunostaining and retrograde labeling of RGCs provide evidence that the effect of MgAT on these molecular events was translated to greater RGC survival. Previous studies have shown that estimation of RGC survival by these two methods show good correlation as was the case in the present study. In the present study, we did not observe the changes in the survival of a distinct class of RGCs, known as intrinsically photosensitive RGCs that are melanopsin positive. However, melanopsin-positive RGCs are fully resistant to NMDA but not the Brn3A-positive RGCs. Thus, use of Brn3A immunolabeling in the present study was more significant [56]. Furthermore, it has been observed that the injury such as that caused by FluoroGold application although may transiently affect the survival of melanopsin-positive RGCs, but the survival of Brn3A-positive RGCs is not affected [57].

Although the inner retina is the primary site of injury in glaucoma, studies have shown involvement of photoreceptors in glaucomatous eyes [58]. Moreover, glutamate is the major neurotransmitter for photoreceptors; thus, NMDA exposure could cause photoreceptor damage and affect the color vision of the animals in the present study. Therefore, color recognition by the animals was assessed to further confirm the protective effects of MgAT.

In an open field, rats may exhibit increased exploratory behavior due to fear of navigating through an unknown space. Rats that can recognize the visual cues are expected to quickly adapt to new space, whereas those with poor vision have to explore longer to adapt. All five parameters (total distance traveled, number of line crossings, frequency of grooming, total immobile time, episodes of immobility, and frequency of rearing) consistently showed greater exploratory behavior among the NMDA-treated rats compared to the MgAT-treated rats, a possible indication of better vision among the MgAT-treated rats. Greater exploratory activity among rats

Table 1. List of primers used is this study.

Gene	Sequence	Gene ID	NCBI Reference
GAPDH	F: ATGATTCTACCCACGGCAAG	81822	NM_031144.3
	R: CTGGAAGATGGTGATGGGTT		
Beta Actin	F: GACATCCGTAAAGACCTCTATGCC	24383	NM_017008.4
	R: ATAGAGCCACCAATCCACACAGAG		
Calpain 1	F: CGACCTCTACCAGATCATTC	29153	NM_019152.2
	R: GTAATAGCCTCCAAATCACG		
Cabin 1	F: ACTCCTATGGGTGATGTTTC	94165	NM_053575.2
	R: CCACTTTCCTCTAAAGTCTTC		
Camk2a	F: AAACAAGAAGAATGATGGCG	25400	NM_012920.1
	R: TTCGTGTAGGATTCAAAGTC		
Camk2b	F: CTAGAGATCACCAGAAGCTG	24245	NM_001042354.1
	R: CCTCACTGTAGTACTCTCTC		
Camk2d	F: GATTTTCCATCACCAGAATGG	24246	NM_012519.2
	R: TTCAAGCAGTCTACAGTCTC		
Camk2g	F: GAAAGATCCCTATGGAAAACC	171140	NM_133605.1
	R: TGGTTGATCAAGTTCTTAGC		

with poor vision has been known for a long time. For the color recognition test in the open-field arena, the rats were first allowed to familiarize themselves with space and color objects so that on subsequent exposure they did not recognize the same objects as novel. Rats have an innate preference for greater exploration of the novel rather than the familiar object. In the present study, object exploration was scored whenever the rat sniffed the object with the distance between the nose and the object less than 2 cm or if the rat touched the object while looking at it. It is a common practice to define the exploratory approach as “directing the nose” toward the object “at a distance less than or equal to 2 cm” and climbing over or leaning on an object without sniffing is not considered an explorative behavior [59]. During trial 1, the rats in all groups exhibited similar exploratory behavior as the objects were recognized as novel. However, during the subsequent trials, the MgAT-treated rats showed significantly less explorations compared to the NMDA-treated rats. Perhaps due to recognition of color cues by the MgAT-treated rats, the objects were not recognized as novel on subsequent exposure. Interestingly, in the displacement and replacement phase the MgAT-treated rats showed less exploratory activity toward the blue object compared to the NMDA-treated rats, but the same was not true for the green object. The reason for this remains unclear. However, a study has shown that within the wavelength range of 300–500 nm (the wavelength increases from ultraviolet to blue to green from 300 to 500 nm), the ability of rats to correctly discriminate colors decreases as the wavelength increases [60]. Thus, it is likely that the green object was not discriminated as clearly as the blue object but was recognized as a novel object. In the Morris water test, the platform was always paired with the blue object, and it was clearly demonstrated that the latency period to find the platform was significantly shorter in the MgAT-treated rats compared to the NMDA-treated rats.

In the protocol for the visual function tests, some of the confounders could not be eliminated in the present study. For example, the viewing distance could not be controlled. The actual distance at which the animals recognized the colors may have varied among groups and could not be accounted for. Whether the visual angle brought about a difference in the visual acuity could not be determined. Additionally, these tasks did not allow assessment of visual functions in one or the other eye as well as the visual acuity. The contribution of spatial memory in the final outcome could not be completely excluded. Despite these limitations, an overall assessment of the animals’ color recognition ability could be made, and clearly, it was demonstrated that the MgAT- pretreated rats had greater retention of color perception compared to the NMDA-treated rats indicating the neuroprotective effects of MgAT against NMDA-induced retinal damage.

In conclusion, the present study showed that MgAT protects against NMDA-induced RGC apoptosis and changes in visual functions in rats. These effects of MgAT were associated with altered retinal gene and protein expression for calpain-1, cabin-1, and CaMKII.

ACKNOWLEDGMENTS

Authors acknowledge the financial support by Ministry of Education under grant number 600-RMI/RAGS 5/3 (40/2014). Authors also acknowledge the facility support by IMMB and LACU, University Teknologi MARA. Our sincere thanks to Prof Alexander Spasov and Prof Alexander Ozerov from Volgograd State Medical University, Research Centre for Innovative Medicines, Volgograd for synthesizing and sending magnesium acetyltaurate for this research work.

REFRENCES

1. 1Quigley HA, Nickells RW, Kerrigan LA, Pease ME, Thibault DJ, Zack DJ. Retinal ganglion cell death in experimental glaucoma and after axotomy occurs by apoptosis. Invest Ophthalmol Vis Sci 1995; 36:774-86. [PMID: 7706025].
2. 2Cordeiro MF, Guo L, Luong V, Harding G, Wang W, Jones HE, Moss SE, Sillito AM, Fitzke FW. Real time imaging of single nerve cell apoptosis in retinal neurodegeneration. Proc Natl Acad Sci USA 2004; 101:13352-6. [PMID: 15340151].
3. 3Osborne NN, Ugarte M, Chao M, Chidlow G, Bae JH, Wood JP, Nash MS. Neuroprotection in relation to retinal ischemia and relevance to glaucoma. Surv Ophthalmol 1999; 43:S102-28. [PMID: 10416754].
4. 4Choi DW. Glutamate neurotoxicity and diseases of the nervous system. Neuron 1988; 1:623-34. [PMID: 2908446].
5. 5Thoreson WB, Witkovsky P. Glutamate receptors and circuits in the vertebrate retina. Prog Retin Eye Res 1999; 18:765-810. [PMID: 10530751].
6. 6Ferreira IL, Duarte CB, Carvalho AP. Ca2+ influx through glutamate receptor-associated channels in retina cells correlates with neuronal cell death. Eur J Pharmacol 1996; 302:153-62. [PMID: 8791003].
7. 7Casson RJ. Possible role of excitotoxicity in the pathogenesis of glaucoma. Clin Experiment Ophthalmol 2006; 34:54-63. [PMID: 16451260].
8. 8Agarwal R, Agarwal P. Rodent models of glaucoma and their applicability for drug discovery. Expert Opin Drug Discov 2017; 12:261-70. [PMID: 28075618].
9. 9Vidal-Villegas B, Di Pierdomenico J, Miralles de Imperial-Ollero JA, Ortín-Martínez A, Nadal-Nicolás FM, Bernal-Garro JM, Cuenca Navarro N, Villegas-Pérez MP, Vidal-Sanz M. Melanopsin+RGCs Are fully Resistant to NMDA-Induced Excitotoxicity. Int J Mol Sci 2019; 20:E3012-[PMID: 31226772].
10. 10Croall DE, DeMartino GN. Calcium-activated neutral protease (calpain) system: structure, function, and regulation. Physiol Rev 1991; 71:813-47. [PMID: 2057527].
11. 11Saido TC, Sorimachi H, Suzuki K. Calpain: new perspectives in molecular diversity and physiological-pathological involvement. FASEB J 1994; 8:814-22. [PMID: 8070630].
12. 12Klee CB, Ren H, Wang X. Regulation of the calmodulin-stimulated protein phosphatase, calcineurin. J Biol Chem 1998; 273:13367-70. [PMID: 9593662].
13. 13Wu HY, Tomizawa K, Oda Y, Wei FY, Lu YF, Matsushita M, Li ST, Moriwaki A, Matsui H. Critical role of calpain-mediated cleavage of calcineurin in excitotoxic neurodegeneration. J Biol Chem 2004; 279:4929-40. [PMID: 14627704].
14. 14Kim MJ, Jo DG, Hong GS, Kim BJ, Lai M, Cho DH, Kim KW, Bandyopadhyay A, Hong YM, Kim DH, Cho C, Liu JO, Snyder SH, Jung YK. Calpain-dependent cleavage of cain/cabin1 activates calcineurin to mediate calcium-triggered cell death. Proc Natl Acad Sci USA 2002; 99:9870-5. [PMID: 12114545].
15. 15Terashima T, Ochiishi T, Yamauchi T. Immunocytochemical localization of calcium/calmodulin-dependent protein kinase II isoforms in the ganglion cells of the rat retina: immunofluorescence histochemistry combined with a fluorescent retrograde tracer. Brain Res 1994; 650:133-9. [PMID: 7953663].
16. 16Griffith LC. Calcium/calmodulin-dependent protein kinase II: an unforgettable kinase. J Neurosci 2004; 24:8391-3. [PMID: 15456809].
17. 17Hajimohammadreza I, Probert AW, Coughenour LL, Borosky SA, Marcoux FW, Boxer PA, Wang KK. A specific inhibitor of calcium/calmodulin-dependent protein kinase-II provides neuroprotection against NMDA- and hypoxia/hypoglycemia-induced cell death. J Neurosci 1995; 15:4093-101. [PMID: 7538570].
18. 18Wright SC, Schellenberger U, Ji L, Wang H, Larrick JW. Calmodulin-dependent protein kinase II mediates signal transduction in apoptosis. FASEB J 1997; 11:843-9. [PMID: 9285482].
19. 19Laabich A, Cooper NG. Neuroprotective effect of AIP on N-methyl-D-aspartate-induced cell death in retinal neurons. Brain Res Mol Brain Res 2000; 85:32-40. [PMID: 11146104].
20. 20Manabe S, Gu Z, Lipton SA. Activation of matrix metalloproteinase-9 via neuronal nitric oxide synthase contributes to NMDA-induced retinal ganglion cell death. Invest Ophthalmol Vis Sci 2005; 46:4747-53. [PMID: 16303975].
21. 21Maekawa S, Sato K, Fujita K, Daigaku R, Tawarayama H, Murayama N, Moritoh S, Yabana T, Shiga Y, Omodaka K, Maruyama K, Nishiguchi KM, Nakazawa T. The neuroprotective effect of hesperidin in NMDA-induced retinal injury acts by suppressing oxidative stress and excessive calpain activation. Sci Rep 2017; 7:6885-[PMID: 28761134].
22. 22Lambuk L, Jafri AJ, Arfuzir NN, Iezhitsa I, Agarwal R, Rozali KN, Agarwal P, Bakar NS, Kutty MK, Yusof AP, Krasilnikova A, Spasov A, Ozerov A, Ismail NM. Neuroprotective Effect of Magnesium Acetyltaurate Against NMDA-Induced Excitotoxicity in Rat Retina. Neurotox Res 2017; 31:31-45. [PMID: 27568334].

23. 23Jafri AJA, Agarwal R, Iezhitsa I, Agarwal P, Spasov A, Ozerov A, Ismail NM. Protective effect of magnesium acetyltaurate and taurine against NMDA-induced retinal damage involves reduced nitrosative stress. Mol Vis 2018; 24:495-508. [PMID: 30090013].

24. 24Jafri AJA, Arfuzir NNN, Lambuk L, Iezhitsa I, Agarwal R, Agarwal P, Razali N, Krasilnikova A, Kharitonova M, Demidov V, Serebryansky E, Skalny A, Spasov A, Yusof APM, Ismail NM. Protective effect of magnesium acetyltaurate against NMDA-induced retinal damage involves restoration of minerals and trace elements homeostasis. J Trace Elem Med Biol 2017; 39:147-54. [PMID: 27908408].

25. 25Arfuzir NN, Lambuk L, Jafri AJ, Agarwal R, Iezhitsa I, Sidek S, Agarwal P, Bakar NS, Kutty MK, Yusof AP, Krasilnikova A, Spasov A, Ozerov A, Mohd Ismail N. Protective effect of magnesium acetyltaurate against endothelin-induced retinal and optic nerve injury. Neuroscience 2016; 325:153-64. [PMID: 27012609].

26. 26Nor Arfuzir NN, Agarwal R, Iezhitsa I, Agarwal P, Sidek S, Spasov A, Ozerov A, Mohd Ismail N. Effect of Magnesium Acetyltaurate and Taurine on Endothelin1-Induced Retinal Nitrosative Stress in Rats. Curr Eye Res 2018; 43:1032-40. [PMID: 29676937].

27. 27Bustin SA, Benes V, Garson JA, Hellemans J, Huggett J, Kubista M, Mueller R, Nolan T, Pfaffl MW, Shipley GL, Vandesompele J, Wittwer CT. The MIQE guidelines: minimum information for publication of quantitative real-time PCR experiments. Clin Chem 2009; 55:611-22. [PMID: 19246619].

28. 28Kirby ED, Jensen K, Goosens KA, Kaufer D. Stereotaxic surgery for excitotoxic lesion of specific brain areas in the adult rat. J Vis Exp 2012; (65)e4079-[PMID: 22847556].

29. 29Yao F, Zhang E, Gao Z, Ji H, Marmouri M, Xia X. Did you choose appropriate tracer for retrograde tracing of retinal ganglion cells? The differences between cholera toxin subunit B and Fluorogold. PLoS One 2018; 13:e0205133-[PMID: 30289890].

30. 30Nadal-Nicolás FM, Salinas-Navarro M, Jiménez-López M, Sobrado-Calvo P, Villegas-Pérez MP, Vidal-Sanz M, Agudo-Barriuso M. Displaced retinal ganglion cells in albino and pigmented rats. Front Neuroanat 2014; 8:99-[PMID: 25339868].

31. 31Maei HR, Zaslavsky K, Teixeira CM, Frankland PW. What is the Most Sensitive Measure of Water Maze Probe Test Performance? Front Integr Nuerosci 2009; 3:4-[PMID: 19404412].

32. 32Morris RGM. Spatial localization does not require the presence of local cues. Learn Motiv 1981; 12:239-60. .

33. 33Vorhees CV, Williams MT. Morris water maze: procedures for assessing spatial and related forms of learning and memory. Nat Protoc 2006; 1:848-58. [PMID: 17406317].

34. 34Nunez J. Morris Water Maze Experiment. J Vis Exp 2008; (19)897-[PMID: 19066539].

35. 35Nakagawa T, Yuan J. Cross-talk between two cysteine protease families. Activation of caspase-12 by calpain in apoptosis. J Cell Biol 2000; 150:887-94. [PMID: 10953012].

36. 36Vosler PS, Brennan CS, Chen J. Calpain-mediated signaling mechanisms in neuronal injury and neurodegeneration. Mol Neurobiol 2008; 38:78-100. [PMID: 18686046].

37. 37Chan SL. Caspase and calpain substrates: roles in synaptic plasticity and cell death. J Neurosci Res 1999; 58:167-90. [PMID: 10491581].

38. 38Hyrc K. Ionized intracellular calcium concentration predicts excitotoxic neuronal death: observations with low-affinity fluorescent calcium indicators. J Neurosci 1997; 17:6669-77. [PMID: 9254679].

39. Hewitt KE, Lesiuk HJ, Tauskela JS, Morley P, Durkin JP. Selective coupling of mu-calpain activation with the NMDA receptor is independent of translocation and autolysis in primary cortical neurons. J Neurosci Res 1998; 54:223-32. [PMID: 9788281].

40. Chiu K, Tim TL, Li WWY, Caprioli J, Kwong JMK. Calpain and N-methyl-D-aspartate (NMDA)-induced excitotoxicity in rat retinas. Brain Res 2005; 1046:207-15. [PMID: 15878434].

41. D'Orsi B, Bonner H, Tuffy LP, Düssmann H, Woods I, Courtney MJ, Ward MW, Prehn JH. Calpains Are Downstream Effectors of bax -Dependent Excitotoxic Apoptosis. J Neurosci 2012; 32:1847-58. [PMID: 22302823].

42. Nicholls DG, Scott ID. The role of mitochondria in the regulation of calcium ion transport in synaptosomes. Biochem Soc Trans 1980; 8:264-6. [PMID: 7399048].

43. Luetjens CM, Bui NT, Sengpiel B, Münstermann G, Poppe M, Krohn AJ, Bauerbach E, Krieglstein J, Prehn JHM. Delayed mitochondrial dysfunction in excitotoxic neuron death: cytochrome c release and a secondary increase in superoxide production. J Neurosci 2000; 20:5715-23. [PMID: 10908611].

44. Dawson TM, Steiner JP, Lyons WE, Fotuhi M, Blue M, Snyder SH. The immunophilins, FK506 binding protein and cyclophilin, are discretely localized in the brain: relationship to calcineurin. Neuroscience 1994; 62:569-80. [PMID: 7530348].

45. Sasaki T, Han F, Shioda N, Moriguchi S, Kasahara J, Ishiguro K, Fukunaga K. Lithium-induced activation of Akt and CaM kinase II contributes to its neuroprotective action in a rat microsphere embolism model. Brain Res 2006; 1108:98-106. [PMID: 16843447].

46. Yamagata Y, Imoto K, Obata K. A mechanism for the inactivation of Ca2/calmodulin-dependent protein kinase II during prolonged seizure activity and its consequence after the recovery from seizure activity in rats in vivo. Neuroscience 2006; 140:981-92. [PMID: 16632208].

47. Goebel DJ. Selective blockade of CaMKII-alpha inhibits NMDA-induced caspase-3-dependent cell death but does not arrest PARP-1 activation or loss of plasma membrane selectivity in rat retinal neurons. Brain Res 2009; 1256:190-204. [PMID: 19135986].

48. Fan W, Agarwal N, Kumar MD, Cooper NG. Retinal ganglion cell death and neuroprotection: Involvement of the CaMKI-Ialpha gene. Brain Res Mol Brain Res 2005; 139:306-16. [PMID: 16023257].

49. Fan W, Agarwal N, Cooper NG. The role of CaMKII in BDNF-mediated neuroprotection of retinal ganglion cells (RGC-5). Brain Res 2006; 1067:48-57. [PMID: 16337157].

50. Fan W, Cooper NG. Glutamate-induced NFkappaB activation in the retina. Invest Ophthalmol Vis Sci 2009; 50:917-25. [PMID: 18836176].

51. Vest RS, O'Leary H, Coultrap SJ, Kindy MS, Bayer KU. Effective postinsult neuroprotection by a novel Ca(2+)/calmodulin-dependent protein kinase II (CaMKII) inhibitor. J Biol Chem 2010; 285:20675-82. [PMID: 20424167].

52. Srinivasan M, Edman CF, Schulman H. Alternative splicing introduces a nuclear localization signal that targets multifunctional CaM kinase to the nucleus. J Cell Biol 1994; 126:839-52. [PMID: 7519621].

53. Brocke L, Chiang LW, Wagner PD, Schulman H. Functional implications of the subunit composition of neuronal CaM kinase II. J Biol Chem 1999; 274:22713-22. [PMID: 10428854].

54. Salas MA, Valverde CA, Sánchez G, Said M, Rodriguez JS, Portiansky EL, Kaetzel MA, Dedman JR, Donoso P, Kranias EG, Mattiazzi A. The signalling pathway of CaMKII-mediated apoptosis and necrosis in the ischemia/reperfusion injury. J Mol Cell Cardiol 2010; 48:1298-306. [PMID: 20060004].

55. Doré K, Labrecque S, Tardif C, De Koninck P. FRET-FLIM investigation of PSD95-NMDA receptor interaction in dendritic spines; control by calpain, CaMKII and Src family kinase. PLoS One 2014; 9:e112170-[PMID: 25393018].

56. Vidal-Villegas B, Di Pierdomenico J, Miralles de Imperial-Ollero JA, Ortín-Martínez A, Nadal-Nicolás FM, Bernal-Garro JM, Cuenca Navarro N, Villegas-Pérez MP. Vidal-Sanz M9. Melanopsin+RGCs are fully resistant to NMDA-induced excitotoxicity. Int J Mol Sci 2019; 20:E3012-[PMID: 31226772].

57. Nadal-Nicolás FM, Madeira MH, Salinas-Navarro M, Jiménez-López M, Galindo-Romero C, Ortín-Martínez A, Santiago AR, Vidal-Sanz M, Agudo-Barriuso M. Transient Downregulation of Melanopsin Expression After Retrograde Tracing or Optic Nerve Injury in Adult Rats. Invest Ophthalmol Vis Sci 2015; 56:4309-23. [PMID: 26176868].

58. Nork TM, Ver Hoeve JN, Poulsen GL, Nickells RW, Davis MD, Weber AJ. Vaegan, Sarks SH, Lemley HL, Millecchia LL. Swelling and loss of photoreceptors in chronic human and experimental glaucomas. Arch Ophthalmol 2000; 118:235-45. [PMID: 10676789].

59. Wilkinson JL, Herrman L, Palmatier MI, Bevins RA, Bevins RA. Rats' novel object interaction as a measure of environmental familiarity. Learn Motiv 2006; 37:31-48. .

60. Jacobs GH, Fenwick JA, Williams GA. Cone-based vision of rats for ultraviolet and visible lights. J Exp Biol 2001; 204:2439-46. [PMID: 11511659].

Articles are provided courtesy of Emory University and the Zhongshan Ophthalmic Center, Sun Yat-sen University, P.R. China. The print version of this article was created on 3 June 2020. This reflects all typographical corrections and errata to the article through that date. Details of any changes may be found in the online version of the article.